Colloquium: The physics of charge inversion in chemical and biological systems

A. Yu. Grosberg, T. T. Nguyen, and B. I. Shklovskii

Department of Physics, University of Minnesota, Minneapolis, Minnesota 55455

(Published 19 April 2002)

The authors review recent advances in the physics of strongly interacting charged systems functioning in water at room temperature. In these systems, many phenomena go beyond the framework of mean-field theories, whether linear Debye-Hückel or nonlinear Poisson-Boltzmann, culminating in charge inversion—a counterintuitive phenomenon in which a strongly charged particle, called a macroion, binds so many counterions that its net charge changes sign. The review discusses the universal theory of charge inversion based on the idea of a strongly correlated liquid of adsorbed counterions, similar to a Wigner crystal. This theory has a vast array of applications, particularly in biology and chemistry; for example, in the presence of positive multivalent ions (e.g., polycations), the DNA double helix acquires a net positive charge and drifts as a positive particle in an electric field. This simplifies DNA uptake by the cell as needed for gene therapy, because the cell membrane is negatively charged. Analogies of charge inversion to other fields of physics are also discussed.

CONTENTS

I. INTRODUCTION

Molecular biological machinery functions in water at around room temperature. For a physicist, this very limited temperature range contrasts unfavorably with the richness of low-temperature physics, where one can change the temperature and scan vastly different energy scales in an orderly manner. In this Colloquium, we review the recently developed understanding of highly charged molecular systems in which Coulomb interactions are so strong that we are effectively in the realm of low-temperature physics.

More specifically, imagine a problem in which one big ion, called a *macroion*, is screened by much smaller but still multivalent ions, each with a large charge Ze, where e is the proton charge; for brevity, we call them Z-ions. A variety of macroions are of importance in chemistry and biology, ranging from the charged surface of mica or charged solid particles to charged lipid membranes, colloids, DNA, actin, and even cells and viruses. Multivalent metal ions, charged micelles, dendrimers, short or long polyelectrolytes including DNA—to name but a few—can play the role of the screening Z-ions.

The central idea of this Colloquium is that of *correlations*: due to strong interactions with the macroion surface and with each other, screening Z-ions do not position themselves randomly in three-dimensional space, but form a strongly correlated liquid on the surface of the macroion. Moreover, in terms of short-range order, this liquid is reminiscent of a Wigner crystal, as Fig. 1 depicts.

Depending on the system geometry and other circumstances, correlations between screening ions may appear in many different ways. To create some simple images in the reader's mind, it is useful to begin with a few examples. One example is that shown in Fig. 1, which could be the surface, say, of a latex particle screened by some compact ions. With a modest leap of the imagination, we could also envision the same picture as the surface of a DNA double helix screened by multivalent counterions, such as spermine with $Z=4$ (Bloomfield, 1996). Here, we imagine DNA as a long, thick cylinder, of diameter 2 nm and charge $-e$ per 1.7 nm along the cylinder, or, in other words, with a huge negative surface charge density $-0.9e/\mathrm{nm}^2$. We study correlations between pointlike Z-ions in Secs. III–V. One obvious problem with the model in Fig. 1 is that it ignores the

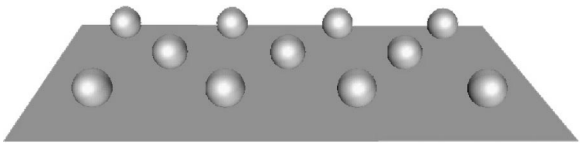

FIG. 1. Strongly correlated liquid—almost a Wigner crystal—of Z-ions on the oppositely charged macroion surface. The figure is characteristic in showing the degree to which we are willing to ignore the microscopic details.

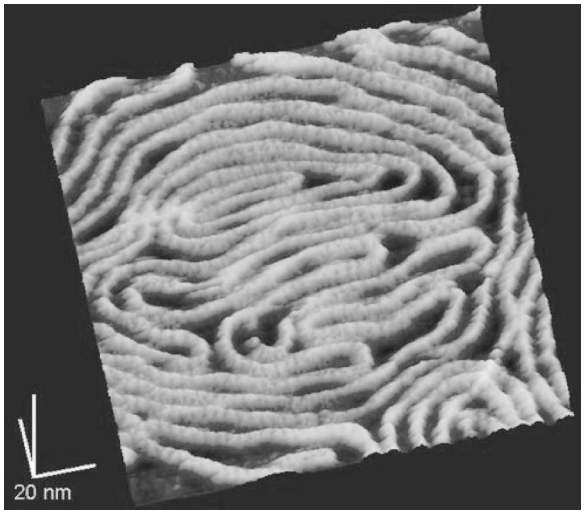

FIG. 2. DNA adsorbed on a positively charged surface, as seen in an atomic force microscopy image (Mou *et al.*, 1995).

discreteness of charges, both in the macroion and in the Z-ions; chemists, for instance, hardly ever accept such continuous models. In Sec. XI, we address the question of electrostatic correlations in systems with discrete charges.

As another example, consider DNA molecules that screen the positive surface charge of a colloid particle or a membrance (Mou *et al.*, 1995; Fang and Yang, 1997). Obviously, DNA chains play the role of Z-ions. For very short DNA pieces, we are back again to Fig. 1, but longer DNA molecules are spaghettilike, and in this situation, correlations mean parallel arrangement, as we see in Fig. 2. Theoretical treatment of this problem in Sec. VI makes a simplifying assumption that this arrangement may be modeled as a system of parallel rods.

Electrostatic correlations are strong, not only for artificial systems involving DNA, but also for the DNA within a cell (Aberts *et al.*, 1994). In particular, to organize DNA in chromatin (in eukariotic cells), Nature uses proteins having large positive charges—histones. Higher levels of chromatin hierarchical structure can be disassembled, with some of the histones released, by an elevated concentration of salt. The resulting most stable lower-level structure is a bead-on-a-string or necklace conformation, as shown in Fig. 3. It is called a 10-nm fiber, because the beads, called nucleosomes, are about that big. Each nucleosome consists of a core particle, called an octamer, with a total charge of about $+170e$. As shown in the inset in Fig. 3, the octamer is encircled 1.8 times by a DNA molecule having a charge of $-292e$. The electrostatic interaction energy between the DNA molecule and the histone octamer dwarfs the bending energy of the DNA molecule. Strikingly, a simple theory discussed in Sec. VII yields a similar structure, Fig. 4, based on purely electrostatic correlations in a simple model.

Correlated screening also has many useful practical applications. Foremost among these is the technology of dressing DNA with polycations (Kabanov and Kabanov, 1995, 1998), positively charged starlike polymers called

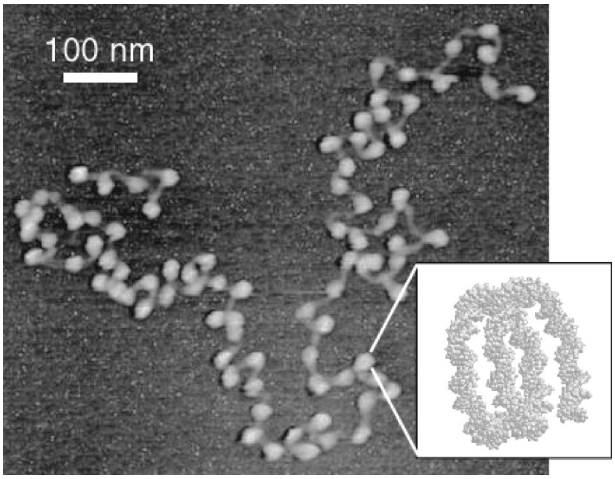

FIG. 3. Electron microscopy image of 10-nm chromatin fiber (Shao, 1999). The beads are nucleosomes. The structure of a nucleosome is known to about 0.2 nm resolution (Luger *et al.*, 1997), and the inset shows how the DNA double helix is bent in the nucleosome. While the overall shape of the fiber is perhaps due to the sample preparation procedure, the array of nucleosomes on the DNA is close to periodic, similar in this respect to the theoretical model shown in Fig. 4.

dendrimers (Tang *et al.*, 1996; Kabanov *et al.*, 2000; Evans *et al.*, 2001), or liposomes (Radler *et al.*, 1997) in order to produce positive complexes with DNA. This facilitates gene delivery through a negative cell surface membrane (Felgner, 1997). There is also the idea of manufacturing nanowires by attaching positive silver or gold colloids to DNA (Braun *et al.*, 1998; Keren *et al.*, 2002).

We view these examples as both important and convincing enough to motivate the study of electrostatic correlations between strongly charged Z-ions. Strong correlations manifest themselves in a number of ways and dramatically alter the entire picture of screening. In the familiar Debye theory, screening somewhat reduces the effective value of charge as seen from a finite distance in the outside world. With strongly correlated ions, overscreening becomes possible, in which case the shielded macroion charge is seen from outside as having the opposite sign. This counterintuitive phenomenon is called *charge inversion*.

The first experimental study related to charge inversion was reported a long time ago by Bungenberg de Jong (1949). More recently, charge-inverted complexes of polyelectrolytes were directly observed in electro-

FIG. 4. Self-assembled complex of a negative polyelectrolyte molecule and many positive spheres in a necklacelike structure. On the surface of a sphere, neighboring polyelectrolyte turns are correlated similar to the rods in Fig. 8 below. On a larger scale, charged spheres repel each other and form a one-dimensional Wigner crystal along the polyelectrolyte molecule.

phoresis experiments (see the review articles of Kabanov and Kabanov, 1995, 1998, and references therein). It is now understood that charge inversion is a generic phenomenon, and it is expected in all systems in which strongly charged ions participate in screening. It turns out to be a natural manifestation of correlations between screening ions. In recent years, the phenomenon of charge inversion has attracted the attention of many theorists.[1]

Another equally interesting manifestation of correlation is the possibility of attraction between like-charged macroions mediated by Z-ions (Rouzina and Bloomfield, 1996; Gronbech-Jensen *et al.*, 1997; Levin *et al.*, 1999; Moreira and Netz, 2001). This has implications in the large field of self-assembly of charged biological objects, ranging from RNA (Pan *et al.*, 1999; Woodson, 2000) to virus heads (Gelbart *et al.*, 2000). In Sec. IX, we show how this attraction of like charges competes with repulsion due to inverted charges, which combine to induce reentrant condensation of DNA or colloids out of solutions.

Although the subject matter of our Colloquium belongs to chemical and biological physics, it has many analogies in other branches of physics, from atomic physics to the quantum Hall effect; we discuss these in Sec. XII.

In what follows, we reexamine the entire concept of screening to include correlations. Although this requires going beyond the mean-field approximation, we shall start with some historical remarks which also serve to define the notations.

II. HISTORICAL REMARKS: MEAN-FIELD THEORIES

The history of our subject goes back almost one hundred years. While we are unable in this brief Colloquium to discuss it in any depth, we shall mention three key steps.

In the first step, Gouy (1910) and, independently, Chapman (1913) examined the double layer at an electrode surface, an intensely disputed subject at the time. Following Gouy and Chapman, let us consider a massive insulating macroion. Assume that its charge is negative, with surface density $-\sigma$. Assume further that the only counterions in the system are those dissociated from the surface. Since a macroion is large, the problem of the counterion distribution near the surface is one dimensional, with both counterion concentration $N(x)$ and electrostatic potential $\phi(x)$ depending on the distance x from the surface. Gouy and Chapman addressed this problem by solving the following equation:

$$\Delta\phi = -\frac{4\pi}{\epsilon} N_s e Z \exp\left[-eZ\frac{\phi(x)-\phi_s}{k_B T}\right]. \tag{1}$$

Here $\epsilon \approx 80$ is the dielectric constant of water, ϕ_s is the potential at the surface, and N_s is the counterion concentration at the surface. Equation (1) follows from the Poisson equation for the potential $\phi(x)$ and the assumption that the ions determining the charge density are Boltzmann distributed in the same potential. Because of this self-consistency assumption, this equation describes a mean-field approximation. It is universally called the Poisson-Boltzmann equation. One boundary condition $d\phi/dx|_{x=0} = 4\pi\sigma/\epsilon$ follows from the fact that the field vanishes on the other side of the boundary (as there is no electrolyte and there are no charges). The second condition is that the concentration $N(x)$ must be normalized to σ/Ze ions per unit area. Thus formulated, the Gouy-Chapman problem allows the simple exact solution

$$N(x) = \frac{k_B T\epsilon/2\pi e^2 Z^2}{(x+\lambda)^2}, \tag{2}$$

where λ is called the Gouy-Chapman length, which is equal to

$$\lambda = k_B T\epsilon/2\pi\sigma Z e. \tag{3}$$

The interpretation of Eq. (3) is interesting. If a Z-ion were to be alone next to the charged plane, it would be confined by the surface field $2\pi\sigma/\epsilon$ to such a "height" λ that its energy change $2\pi\sigma Ze\lambda/\epsilon$ would be about $k_B T$—which leads to the correct answer in Eq. (3). Other Z-ions cancel the field inside the macroion but double the field in the electrolyte at the macroion surface (see above for the boundary condition at $x=0$). On the other hand, every particular ion at every moment is higher than roughly half of the other ions, whereupon it finds itself in a partially screened field. An exact solution of the Poisson-Boltzmann equation indicates that these two factors cancel each other, yielding Eq. (3).

The next step in the screening story, well known to every physicist, is the theory of Debye and Hückel (1923), initially developed for electrolytes—the overall neutral mixture of mobile ions of both signs—and now widely used in plasma and solid-state physics. Debye and Hückel linearized the Poisson-Boltzmann equation (1) (generalized by introducing the sum over ion species on the right-hand side). Of course, linearization can be done if the potential is not too strong anywhere in the system, which is often the case if the charges involved are small enough. Debye-Hückel screening leads to exponential decay of the potential around a pointlike charge Q:

$$\phi(r) = \frac{Q}{\epsilon r} e^{-r/r_s}, \tag{4}$$

where the Debye-Hückel radius is given by

[1] See, for example, Ennis *et al.*, 1996; Wallin and Linse, 1996, 1997; Joanny, 1999; Matcescu *et al.*, 1999; Netz and Joanny, 1999a; Park *et al.*, 1999; Perel and Shklovskii, 1999; Sens and Gurovich, 1999; Shklovskii, 1999b; Wang *et al.*, 1999; Andelman and Joanny, 2000; Messina *et al.*, 2000a, 2000b; Nguyen *et al.*, 2000a, 2000b; Chodanowski and Stoll, 2001; Dobrynin *et al.*, 2001; Nguyen and Shklovskii, 2001a, 2001b, 2001c, 2001d, 2001e; Potemkin *et al.*, 2001; Tanaka and Grosberg, 2001a.

$$r_s=\left(\frac{k_BT\epsilon}{8\pi N_1e^2}\right)^{1/2}, \tag{5}$$

and N_1 is the concentration of monovalent salt.

Less well known among physicists is the fact that the Debye-Hückel theory ignited a heated debate: Bjerrum (1926) commented that $\int \exp[e^2/rk_BT]r^2dr$ diverges at $r\to 0$, and therefore pointlike charged particles are expected to associate in neutral pairs. The discussion led to the realization of the important role of short-range repelling forces. In order to prevent the association of monovalent ions and formation of Bjerrum pairs, the repulsion forces should take over at a distance not much smaller than the so-called Bjerrum length,

$$l_B=e^2/\epsilon k_BT, \tag{6}$$

which is about 0.7 nm in water at room temperature. (This is why the hydration layer of a few water molecules around each ion is essential to stabilize dissociated ions.)

The last step we mention here is relatively recent; it has to do with nonlinear screening of cylindrical charges, such as the DNA double helix (Onsager, 1967; Manning, 1969; Oosawa, 1971). Consider a cylinder charged to the linear density $-\eta$. Since the potential is logarithmic, its competition with entropy is quite peculiar. Indeed, releasing counterions to some distance r requires energy $(2eZ\eta/\epsilon)\ln(r/a)$, where a is the cylinder radius, while the corresponding entropy gain is $k_BT\ln(\pi r^2/\pi a^2)$. Therefore counterions are released only as long as $\eta<\eta_Z$, where

$$\eta_Z=k_BT\epsilon/eZ. \tag{7}$$

When a cylinder is charged in excess of $-\eta_Z$, some of the ions remain *Onsager-Manning condensed* on the cylinder, so that its effective net charge is equal to $-\eta_Z$. To emphasize the importance of this subject, let us mention that the DNA double helix has a bare charge density of about $-4.2\eta_1$, where $\eta_1=\eta_Z|_{Z=1}$ [see Frank-Kamenetskii *et al.* (1987) for further DNA applications]. Onsager-Manning condensation was more accurately justified by Zimm and Le Bret (1983). These authors addressed the nonlinear Poisson-Boltzmann equation in cylindrical geometry (refining earlier works—see the collection of papers by Katzir-Katchalsky, 1971).

The Gouy-Chapman, Debye-Hückel, and Onsager-Manning theories are all of the mean-field type, based on the Poisson-Boltzmann equation. This approach works well when screening charges are small, $Z=1$. In the case of strongly charged macroions and Z-ions, however, correlations are important and mean-field theory fails. Hence it is necessary to go beyond this approximation. This is precisely the subject matter of the present Colloquium. Charge inversion in this context should be viewed as the most obvious manifestation of the failure of the mean-field approximation.

III. STRONGLY CORRELATED LIQUID OF MULTIVALENT IONS

To begin with, let us explain why the Gouy-Chapman solution (2) fails at large Z. Apart from λ (3), there is a second length scale in the problem due to the discreteness of charge. It is associated with the distance between ions in the lateral direction, that is, along the plane. As long as the system as a whole is neutral, the two-dimensional concentration of Z-ions is $n=\sigma/Ze$, and the surface area per ion can be characterized by a radius R such that $\pi R^2=1/n$ (see Fig. 5). Thus $R=(\pi n)^{-1/2}=(Ze/\pi\sigma)^{1/2}$, and hence [cf. Eq. (3)]

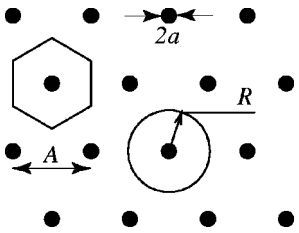

FIG. 5. A Wigner crystal of positive Z-ions on a uniform background of negative surface charge. A hexagonal Wigner-Seitz cell and its simplified version as a disk with radius R are shown.

$$\frac{R}{\lambda}=2\Gamma,\quad \Gamma=\frac{Z^2e^2/\epsilon R}{k_BT}. \tag{8}$$

Here Γ is the Coulomb coupling constant, or the inverse, dimensionless temperature measured in the units of a typical interaction energy between Z-ions. A system of monovalent ions, $Z=1$, is weakly coupled, $\Gamma\sim 1$, and this is why classical mean-field theory applies. By contrast, a system in which Z-ions have large Z is strongly coupled, and we see that R becomes larger than λ. For example, at $Z=3$ and $\sigma=1.0e/\mathrm{nm}^2$, we get $\Gamma=6.4$, $\lambda\simeq 0.1$ nm, and $R\simeq 1.0$ nm. Clearly, mean-field treatment along the lines of Poisson-Boltzmann theory fails in this situation, since Z-ions do not affect each other when they are at distances smaller than R from the plane. It is worth emphasizing once again that it is not only the *linearized* Debye-Hückel theory that fails in the strong-coupling regime; the *nonlinear* Poisson-Boltzmann theory also fails. It is the mean-field approximation that is inapplicable because of correlations between discrete charges.

An alternative theory appropriate for the regime $\Gamma\gg 1$ was suggested by Perel and Shklovskii (1999). The main idea of this theory is that at $\Gamma\gg 1$ the screening atmosphere is narrowly confined at the surface (see Fig. 1), and it should be approximated as a two-dimensional strongly correlated liquid.

A two-dimensional liquid of classical charged particles on a neutralizing background, the so-called one-component plasma, is well understood (Totsuji, 1978). At zero temperature, it acquires the minimal energy state of a Wigner crystal, shown in Fig. 5, in which the correlation energy per ion and the chemical potential are given by

$$\varepsilon(n)\simeq -1.11Z^2e^2/R\epsilon=-1.96n^{1/2}Z^2e^2/\epsilon, \tag{9}$$

$$\mu_{WC}=\frac{\partial[n\varepsilon(n)]}{\partial n}=\frac{3}{2}\varepsilon(n)=-1.65Z^2e^2/\epsilon R. \tag{10}$$

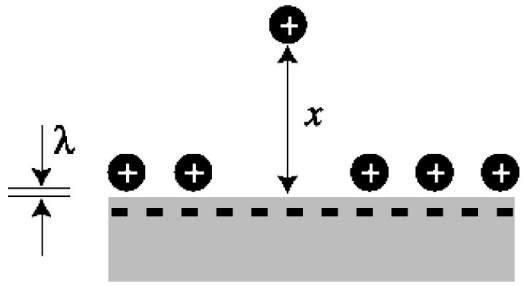

FIG. 6. The origin of attraction of a new positive Z-ion to the already neutralized surface. Z-ions are shown by solid circles. The new Z-ion creates its negative correlation hole.

We interpret R here as the radius of a Wigner-Seitz cell approximated by a disk (see Fig. 5).

At nonzero temperature, the chemical potential of a one-component plasma can be written as $\mu=\mu_{id}+\mu_{WC}+\delta\mu$. Here μ_{id} is the chemical potential of an ideal gas at the same concentration. Accordingly, the $\mu_{WC}+\delta\mu$ part is entirely due to correlations. Furthermore, it turns out that $\delta\mu$, which is the thermal correction, is negligible for $\Gamma\gg1$. Although a Wigner crystal, in terms of long-range order, melts at $\Gamma\approx130$, the value of $\delta\mu$ is controlled by short-range order and remains negligible as long as $\Gamma\gg1$. It is in this sense that a strongly correlated liquid of Z-ions is similar to a Wigner crystal.

Thus the correlation part of the chemical potential can be approximated by μ_{WC} (10), which is negative and large: $-\mu_{WC}/k_BT=1.65\Gamma\gg1$. The physics of a large and negative μ_{WC} can be understood as follows. Pretend for a moment that the insulating macroion is replaced by a neutral metallic surface. In this case, each Z-ion creates an image charge of opposite sign inside the metal. The energy of attraction to the image is $U(x)=-(Ze)^2/4\epsilon x$, where x is the distance to the surface. This energy is minimal when the Z-ion is placed next to the surface, at a distance equal to its radius a; therefore, the Z-ion sticks to the surface. With this idea in mind, consider bringing a new Z-ion to the insulating macroion surface already covered by an adsorbed layer of Z-ions (Fig. 6). This layer behaves like a metal surface in the sense that the new Z-ion repels adsorbed ones, creating a correlation hole. In other words, it creates a negative image. Because of the discreteness of charges, the adsorbed layer is a good metal at length scales above R only. Accordingly, attraction to the image gets saturated at $x\sim R$. This is why the chemical potential of an ion in a Wigner crystal scales as $\mu_{WC}\sim-(Ze)^2/\epsilon R$. Equation (10) specifies the numerical coefficient in this expression.

Using images, we can now understand the distribution of Z-ions, $N(x)$, near the surface. To do this, let us extract one Z-ion from the strongly correlated liquid and move it along the x axis. As long as $x\ll R$, its correlation hole does not change, and, therefore, the Z-ion is attracted to the surface by the uniform electric field $E=2\pi\sigma/\epsilon$; other Z-ions do not affect this attraction in any way. Therefore $N(x)=N_s\exp(-x/\lambda)$ for $x\ll R$. Here $N_s\simeq n/\lambda$ is the three-dimensional concentration of Z-ions close to the surface plane [Eq. (1)]. For $x\gg R$, the correlation hole acts as a pointlike image charge, the corresponding interaction energy being $-Z^2e^2/4\epsilon x$. At $x=Z^2e^2/4\epsilon k_BT=R_0\Gamma/4=\lambda\Gamma^2/2$, the interaction with the image charge drops to about k_BT, that is, negligible, and the Z-ion concentration becomes

$$N_0=N_s\exp\left(-\frac{|\mu_{WC}|}{k_BT}\right)=N_s\exp\left(-\frac{1.65Z^2e^2}{\epsilon Rk_BT}\right). \quad (11)$$

We shall further comment on the physical meaning of N_0 after Eq. (12). Note that the correction term $-Z^2e^2/4\epsilon x$ to the Z-ion energy, which is important in the interval $R\ll x\ll\lambda\Gamma^2/2$, is similar to the "image" correction to the work function of a metal (Lang, 1973).

The dramatic difference between the exponential decay of $N(x)$ and the Gouy-Chapman $1/(\lambda+x)^2$-law (2) is due to correlation effects. Moreira and Netz (2000) rederived these results in a more formal way and confirmed them by Monte Carlo simulations. Recently, Moreira and Netz (2002) also showed that discreteness of the surface charge neglected above leads to the lateral pinning of Z-ions. This brings Z-ions even closer (somewhat) to the surface. The general direction of this effect can be understood from the limit (although unrealistic for a strongly charged surface) when the distance of closest approach between a discrete surface charge and a Z-ion is so small that they form isolated Bjerrum pairs [see Eq. (6)].

At larger x, correlations and interactions with image charges are unimportant, and the Poisson-Boltzmann equation applies. In this region $N(x)$ varies so smoothly that $N(x)=N_0$ provides an effective boundary condition for the Poisson-Boltzmann equation (Shklovskii, 1999b). At this stage we must remember that in a real physical situation there is always some concentration of Z-ions, N, in the surrounding solution. It can be either larger or smaller than N_0. In the latter case, the surface is overcharged, as we show in Sec. IV below.

IV. CORRELATION-INDUCED CHARGE INVERSION

Let us return once again to the physical argument illustrated by Fig. 6. It explains why an extra Z-ion may be attracted to the macroion surface despite the fact that the surface is already neutralized by the previously adsorbed Z-ions. What happens if another Z-ion approaches? Clearly, the correlation effect will keep providing an attractive force for this and subsequent Z-ions, but it will have to compete with the repulsive force, which is simply due to the fact that the macroion already has too many adsorbed Z-ions and therefore the whole complex is positively charged. Thus the question is this: what is the *equilibrium* amount of (over)charge?

One useful way to think about this is to realize that the correlation mechanism provides voltage to drive overcharging, but the actual amount of (over)charge depends on both voltage and capacitance. Since the latter depends strongly on the geometry, we shall have to explore several cases—macroions that are spherical, cylindrical, etc.

An equivalent view involves the comparison of chemical potentials of adsorbed Z-ions and Z-ions in the bulk solution. This approach immediately suggests that, in equilibrium, the total charge Q^* depends on the concentration N of Z-ions in the surrounding bulk solution. Here Q^* is the net charge of the entire complex, which includes the bare charge of the macroion, $-Q<0$, and the proper (determined by the equilibrium condition) number of adsorbed Z-ions each with charge $Ze>0$.

Let us see now how we can implement the condition of equal chemical potentials for the case of a spherical macroion with radius r. Regarding adsorbed Z-ions, we argue[2] that their chemical potential is only different from the one-component plasma expression (10) by the energy of the Z-ion in the potential $\psi(0)=Q^*/\epsilon r$ created by the net charge Q^*. Therefore the equilibrium condition reads $\mu_{id}+\mu_{WC}+Ze\psi(0)=\mu_b$, where μ_b is the bulk chemical potential. To determine Q^* from here, we first note that $\mu_{id}-\mu_b=k_BT\ln(N_s/N)$; we further express μ_{WC} in terms of N_0 [see Eq. (11)], and finally obtain

$$Q^*=\frac{\epsilon r}{Ze}k_BT\ln(N/N_0). \tag{12}$$

Clearly, the net charge Q^* is indeed positive when $N>N_0$, i.e., it has a sign opposite to the bare charge Q.

The result (12) also sheds light on the meaning of the quantity N_0 defined above, in Eq. (11): this is the concentration of Z-ions in the surrounding bulk solution at which the macroion is exactly neutralized by the adsorbed Z-ions. This concentration is very small because $|\mu_{WC}|/k_BT\gg 1$. For example, $N_0=0.3$ mM and 0.8 μM for $Z=3$ and 4, respectively ($1\ \mathrm{M}\approx 6\times 10^{20}\ \mathrm{cm}^{-3}$). Therefore it is easy to achieve charge inversion by increasing N. How large can Q^* be? At large enough N, translational entropy terms $\mu_b-\mu_{id}$ become negligible compared to μ_{WC}, yielding

$$Q^*/\epsilon r=\psi(0)=|\mu_{WC}|/Ze. \tag{13}$$

Expressing R and $|\mu_{WC}|$ through Q and Z with the help of Eq. (10) (and remembering that $\sigma^*=-\sigma+Zen$), Shklovskii (1999b) arrived at a prediction for the *maximal* inverted charge for a spherical macroion which can be achieved by increasing the concentration of Z:1 salt:

$$Q^*=0.83\sqrt{QZe}. \tag{14}$$

This charge is much larger than Ze, but is still smaller than Q because of limitations imposed by the large charging energy. For example, for $Q=100e, Z=4$, we get $Q^*=17e$. Equation (14) was recently confirmed by numerical simulations (Messina *et al.*, 2000a, 2000b; Tanaka and Grosberg, 2001a). Further increase of charge inversion beyond the level dictated by Eq. (14) is achievable with the help of a monovalent salt (see Sec. V).

In cylindrical geometry, similar arguments lead to a revision of the conventional Onsager-Manning condensation theory (Sec. II) when dealing with multivalent Z-ions. Consider a cylinder with a negative linear charge density $-\eta$ and assume that $\eta>\eta_Z$. Mean-field Onsager-Manning theory (7) predicts $\eta^*=-\eta_Z$. By contrast, Perel and Shklovskii (1999) showed that a correlation-induced negative chemical potential μ_{WC} results in

$$\eta^*=-\eta_Z\frac{\ln(N_0/N)}{\ln(4/\pi Z^6 N l_B^3)}, \tag{15}$$

where l_B is the Bjerrum length (6). This result reproduces the Onsager-Manning one (7) only at extremely small values of N, which are unrealistic at $Z\geqslant 3$. On the other hand, at $N=N_0$ the net charge flips sign, resulting in charge inversion at $N>N_0$ (which is absent in Onsager-Manning theory). At large enough N, the inverted charge density η^* can reach $k_BT\epsilon/e=\eta_1$.

V. ENHANCEMENT OF CHARGE INVERSION BY A MONOVALENT SALT

Most water solutions, particularly biological ones, contain significant amounts of monovalent salt, such as NaCl. Correlations between these monovalent ions are negligible and therefore their only role is to provide Debye-Hückel screening with a decay length r_s (5). This screening makes charge inversion substantially stronger. Indeed, screening by a monovalent salt diminishes the charging energy of the macroion much more than the correlation energy of Z-ions. Furthermore, in a sufficient concentration of salt, the macroion is screened at a distance smaller than its size. Then the macroion can be thought of as an overscreened surface, with an inverted charge Q^* proportional to the surface area. In this sense, the overall shape of the macroion is irrelevant, at least to a first approximation. Therefore we consider here a simpler case: screening of a planar macroion surface with a negative surface charge density $-\sigma$ by a solution with a concentration N of Z:1 salt and a large concentration N_1 of a monovalent salt.

Nguyen *et al.* (2000a) calculated analytically the dependence of the charge-inversion ratio σ^*/σ on r_s in two limiting cases, $r_s\gg R_0$ and $r_s\ll R_0$, where $R_0=(\pi\sigma/Ze)^{-1/2}$ is the radius of a Wigner-Seitz cell at the neutral point $n=\sigma/Ze$. At $r_s\gg R_0$ the calculation starts from Eq. (13). The electrostatic potential of a plane with a charge density σ^* screened at the distance r_s reads

[2]The argument goes as follows. The spherical surface of the macroion has a bare surface charge density $-\sigma=-Q/4\pi r^2$. Let us pretend to place there, along with real charge $-\sigma$, two imaginary spheres with uniform charge densities $\sigma^*=Q^*/4\pi r^2$ and $-\sigma^*$. Their total charge is zero, so they have no effect. However, we can now think of the Z-ions as adsorbed on the sphere with the charge density $-\sigma-\sigma^*$, and with this sphere they form a *neutral* strongly correlated liquid, quite like that considered in Sec. III. The remaining sphere has the charge density σ^* and creates a spherically symmetric field with potential on the surface $\psi(0)$. We emphasize that the macroscopic net charge σ^* does not interact with the one-component plasma, because the potential $\psi(0)$ is constant along the surface, while a one-component plasma is neutral.

$\psi(0)=4\pi\sigma^* r_s$. At $r_s \gg R_0$ screening by monovalent ions does not change Eq. (10) substantially, so that we still can use it in Eq. (13), which now describes charging of a plane capacitor by voltage $|\mu_{WC}|/Ze$. This gives

$$\sigma^*/\sigma = 0.41(R_0/r_s) \ll 1 \quad (r_s \gg R_0). \tag{16}$$

Thus at $r_s \gg R_0$ inverted charge density grows with decreasing r_s.

Now we switch to the case of strong screening by a monovalent salt. To begin, let us assume that screening is already so strong that $r_s \ll R_0$, but the energy of a strongly correlated liquid is still much greater than $k_B T$ per Z-ion. In this regime, the free energy consists of the Debye-Hückel-screened, nearest-neighbor repulsion energies of Z-ions and the attraction energy of the Z-ions to the charged surface:

$$F = (3nZ^2e^2/\epsilon A)\exp(-A/r_s) - 4\pi\sigma r_s Zen/\epsilon, \tag{17}$$

where $A=(2/\sqrt{3})^{1/2}n^{-1/2}$ is the lattice constant of the hexagonal Wigner crystal (Fig. 5). Minimizing F with respect to n, one arrives at

$$\frac{\sigma^*}{\sigma} = \frac{\pi}{2\sqrt{3}}\left(\frac{R_0}{r_s \ln(R_0/r_s)}\right)^2 \quad (r_s \ll R_0). \tag{18}$$

Thus σ^*/σ grows with decreasing r_s and can become larger than 100%. At $r_s \sim R_0$, Eqs. (16) and (18) match each other. As we see, σ^* continues to grow with decreasing r_s. This is because the repulsion between Z-ions becomes weaker, so that it is easier to pack more Z-ions on the surface. Of course, when r_s decreases even further, the binding energy of the Z-ions becomes small, the strongly correlated liquid dissolves, and charge inversion disappears.

The results above are in good agreement with simulations. Terao and Nakayama (2001) reported the results of a Monte Carlo simulation for the system consisting of a macroion with charge $Q=20e$ surrounded by 20 monovalent counterions and 1500 ions of 2:1 electrolyte. Tanaka and Grosberg (2001a) performed molecular dynamics simulations with a spherical macroion of charge $Q=-28e$, spherical Z-ions ($2 \leqslant Z \leqslant 7$), and up to 500 monovalent ions; the system is neutral overall, which determines the number of Z-ions to be between 180 and 52. Simulations confirmed the strong adsorption of the overcharging amount of Z-ions on the surface of the macroion. On a more quantitative level, Tanaka and Grosberg (2001a) examined the dependence of the inverted charge on the ionic strength, I, and found the crossover between $Q^* \propto \sqrt{I} \propto 1/r_s$ and $Q^* \propto I \propto 1/r_s^2$, which is consistent with Eqs. (16) and (18). Tanaka and Grosberg (2001a) attempted also to maximize the charge-inversion ratio Q^*/Q. In agreement with the theoretical views presented above, the growth of charge inversion is capped when correlations between Z-ions are suppressed. We have mentioned the eventual reduction of correlations for a large monovalent salt concentration, or small r_s, when the strongly correlated liquid evaporates. If one tries to increase Z instead of lowering r_s, then, at large Z, correlations become suppressed because monovalent ions condense on Z-ions, forming Z'-ions with smaller net charge Z'. This effect can be clearly seen in Fig. 7 [see Nguyen *et al.* (2000b) for the conditions under which this phenomenon is and is not important]. Nevertheless, Q^*/Q up to about 150% is easily observed.

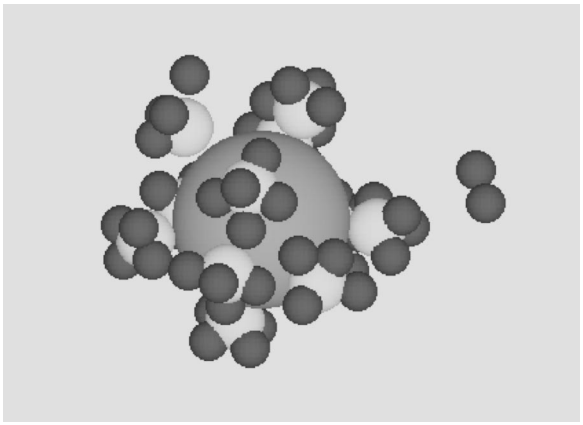

FIG. 7. A snapshot of the system simulated by Tanaka and Grosberg (2001a). The spherical macroion is gray, Z-ions are white, and monovalent negative ions are black. The bare charge of the spherical macroion is $Q=-28e$, $Z=7$, and $\Gamma \approx 30$. There are 52 Z-ions and 336 monovalent ions in the simulation domain. What is clearly seen is the formation of Z'-ions: because Z is so large, Z-ions adsorb monovalent ions. This reduces correlations between Z-ions and restricts charge inversion. Nevertheless, the bare charge of the complex shown in the figure is $+16e$.

VI. SCREENING OF A CHARGED PLANE BY POLYELECTROLYTES

An important class of Z-ion for applications is that of the charged polymers, i.e., polyelectrolytes. Let us start with a rigid polyelectrolyte and discuss charge inversion caused by adsorption of long rodlike Z-ions. For example, the moderately long (up to about 50 nm, or about 150 base pairs) DNA double helix can be well approximated as a rod. Actin is another example of an even more rigid polyelectrolyte. Apart from the uninteresting regime of extremely small macroion surface charge density (in which case the elongated shape of the molecules is irrelevant, rendering our previous results applicable), charged rods adsorbed at the surface tend to be parallel to each other due to their strong lateral repulsion. In other words, there is the short-range order of a one-dimensional Wigner crystal with lattice constant A in the direction perpendicular to the rods (Fig. 8).

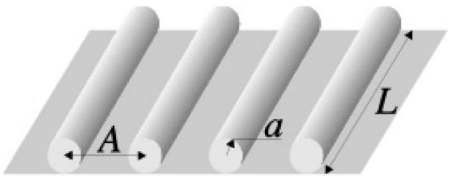

FIG. 8. Rodlike negative Z-ions adsorbed on a positive uniformly charged plane.

To make the signs consistent with the case of DNA, we assume that the polyelectrolyte charge is negative and equal to $-\eta$ per unit length, while the macroion surface is a plane with positive charge density σ. We also assume that there is a certain concentration of monovalent salt, N_1, in the solution, corresponding to the Debye screening radius (5). To begin, let us assume that the charge density of the rods, $-\eta$, is below the Onsager-Manning threshold, Eq. (7), and let us apply the Debye-Hückel approximation to describe the screening of the charged surface by the monovalent salt. We can then directly minimize the free energy of the one-dimensional crystal of negative rods on the positive surface written similarly to Eq. (17). The competition between the attraction of the rods to the surface and the repulsion of the neighboring rods results in a negative net surface charge density $-\sigma^*$ similar to Eq. (18) (Netz and Joanny, 1999a; Nguyen *et al.*, 2000a):

$$\frac{\sigma^*}{\sigma}=\frac{\eta/\sigma r_s}{\ln(\eta/\sigma r_s)}, \quad r_s \ll A_0. \tag{19}$$

Here the applicability condition involves $A_0=\eta/\sigma$, which is the distance between rods when they neutralize the plane; only at $r_s \ll A_0$ is the overcharged plane linearly screened by monovalent salt.

When discussing DNA in Sec. II, we have already mentioned that the DNA charge density $-\eta$ is such that about three-quarters of it is compensated by positive Onsager-Manning-condensed monovalent ions. In other words, the net charge of DNA in the bulk solution is $\eta^*=-\eta_1$ (7). It turns out that, at $r_s \ll A_0$, the result (19) applies to DNA with the sole correction of replacing $-\eta$ with $\eta^*=-\eta_1 \equiv -k_BT\epsilon/e$ (Nguyen *et al.*, 2000a).

Thus the inversion ratio grows with decreasing r_s, as in the case of spherical Z-ions. At small enough r_s and σ, the inversion ratio can reach 200% before DNA molecules are released from the surface. This is larger than for spherical ions, because in this case, due to the great length of the DNA helix, the correlation energy remains large and the Wigner-crystal-like short-range order is preserved at smaller values of σr_s. Nguyen *et al.* (2000a) called this phenomenon "giant charge inversion."

Let us switch now to the opposite extreme of weak screening by a monovalent salt, $r_s \gg A_0$. In this case, screening of the overcharged plane by monovalent salt becomes strongly nonlinear, with the Gouy-Chapman screening length $\lambda^*=\epsilon k_BT/(2\pi e\sigma^*)$, which is much smaller than r_s. Furthermore, some of the positive monovalent ions Onsager-Manning condensed on DNA are released from it upon adsorption, as the plane repels them (Park *et al.*, 1999; Gelbart *et al.*, 2000). As a result, the absolute value of the net linear charge density of each adsorbed DNA, η^*, becomes larger than η_1. To determine σ^* and η^*, Nguyen *et al.* (2000a) considered two equilibrium conditions, dealing with chemical potentials of rods and small ions, respectively. They arrived at the following formulas valid at $r_s \gg A_0$:

$$\frac{\sigma^*}{\sigma}=\frac{\eta_1}{2\pi a\sigma}\exp\left(-\sqrt{\ln\frac{r_s}{a}\ln\frac{A_0}{2\pi a}}\right), \tag{20}$$

$$\eta^*=\eta_1\sqrt{\frac{\ln(r_s/a)}{\ln(A_0/2\pi a)}}, \quad r_s \gg A_0. \tag{21}$$

At $r_s \simeq A_0/2\pi$ we get $\eta^* \simeq \eta_1$, $\lambda^* \simeq r_s$, and $\sigma^*/\sigma \simeq \eta_1/(2\pi r_s\sigma)$, so that Eq. (20) crosses over smoothly to the strong-screening result of Eq. (19).

So far in this section we have assumed a rodlike polyelectrolyte. Let us now discuss how chain flexibility affects charge inversion. We argue that the results for rodlike Z-ions are remarkably robust. For example, consider a polyelectrolyte having several charged groups per each persistence length. We maintain that our results remain valid as long as the adsorption energy *per one persistence length* is large compared to k_BT. Indeed, under this condition even flexible polyelectrolyte chains lie flat on the surface, in which case they are ordered in a Wigner-crystal-like strongly correlated liquid and therefore behave similarly to rods.

Dobrynin *et al.* (2001) addressed the opposite extreme, namely, weakly charged polyelectrolytes, with so small a fraction of charged monomers f that a link between two neighboring charges is already a flexible polymer; in other words, the distance between charges is larger than the persistence length. It was discovered by de Gennes *et al.* (1976) that a weakly charged polyelectrolyte chain in a bulk solution consists of electrostatic blobs. Inside each blob the polymer is only marginally perturbed by Coulomb interactions, while a chain of blobs is fully stretched and rodlike. Dobrynin *et al.* (2001) have found that this blob structure remains valid for the adsorbed chains, which form a strongly correlated liquid of effective rods of blobs. In terms of charge inversion, this means that Eq. (19) remains valid for the weakly charged chains, provided η is replaced with a linear charge density of the string of blobs $\eta^*=(f\epsilon\epsilon k_BT/l^2)^{1/3}$, where l is the chain persistence length and r_s is larger than a blob size.

With increasing σ, adsorbed rods, either real or made of blobs, start to touch each other, leading to multilayer adsorption. It is only in this regime that the real and blob rods behave differently, as we discuss in Sec. VIII.

VII. POLYELECTROLYTES WRAPPING AROUND CHARGED PARTICLES

As we have mentioned in the Introduction, one of the important practical situations is that of a long charged polymer forming complexes with oppositely charged particles. Wallin and Linse (1996, 1997), Mateescu *et al.* (1999), Park *et al.* (1999), Sens and Gurovich (1999), and Netz and Joanny (1999b) considered the complex of a positive sphere with charge q and a negative polyelectrolyte, such as a DNA double helix, which has to make some $n_t>1$ turns around the sphere to neutralize it (Fig. 9). These authors predicted a substantial charge inversion: more of the polyelectrolyte is wound than is necessary to neutralize the sphere. Furthermore, Mateescu *et al.* (1999) found that a tightly coiled polyelectrolyte conformation becomes unstable when the chain length

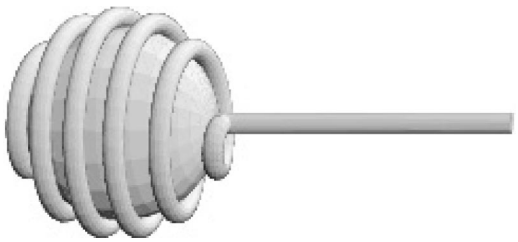

FIG. 9. A polyelectrolyte molecule winding around a spherical macroion. Due to Coulomb repulsion, neighboring turns, which play the role of Z-ions, are strongly correlated.

exceeds a certain threshold and then abruptly stretches out in an almost straight tail (Fig. 9).

Nguyen and Shklovskii (2001a) emphasized the role of correlations in this case of charge inversion. Indeed, neighboring turns repel each other and form an almost equidistant solenoid, which locally resembles a strongly correlated liquid. The tail of the polyelectrolyte repels the already-adsorbed part of the polyelectrolyte and creates a correlation hole, which attracts the tail back to the surface (compare Fig. 6). As a result, the net charge of the sphere with wrapped polyelectrolyte q^* is negative. It is shown that at $r_s \to \infty$ the charge inversion ratio scales as $|q^*|/q \sim 1/n_t$. On the other hand, at small enough r_s it can exceed 100%.

Even more interesting is the system in which the charged polymer is so long that it forms complexes with many oppositely charged particles (see Fig. 4). Examples include micelles (Wang *et al.*, 1999), globular proteins (Kabanov *et al.*, 1976; Xia and Dubin, 1994), colloids (Braun *et al.*, 1998; Keren *et al.*, 2001), dendrimers (Kabanov *et al.*, 2000; Evans *et al.*, 2001), and, last but not least, histone octamers forming 10-nm chromatin fiber with DNA (Fig. 3). To be specific, we remain with the signs consistent with the DNA case and consider a long negative polymer chain in a solution of positive spheres. If the concentration of spheres is large, many spheres adsorb on the polyelectrolyte chain. As a result, each sphere is underscreened by polyelectrolyte and has a positive net charge. Then, adsorbed spheres repel each other and the complex forms a periodic necklace (see Fig. 4). This necklace is, in fact, a one-dimensional Wigner crystal, or strongly correlated liquid, of spheres, which serve as Z-ions. Indeed, since the segment of the polyelectrolyte wound around one sphere interacts almost exclusively with this sphere, it plays the role of a Wigner-Seitz cell. Because of correlations, spheres bind to polyelectrolyte in such a large number that the net charge of the polyelectrolyte molecule becomes positive (Nguyen and Shklovskii, 2001b). In this case, the charge-inversion ratio scales as $Q^*/Q \sim n_t^{1/4}$ in the absence of a monovalent salt, where $-Q$ and Q^* are the bare and net charges of the polyelectrolyte molecule, respectively. This means that charge inversion may be larger than 100%. As we discussed in Sec. V, charge inversion can be further enhanced by a monovalent salt, in which case $Q^*/Q \sim n_t$. We shall return to complexes composed of a charged chain with spheres in Sec. IX.

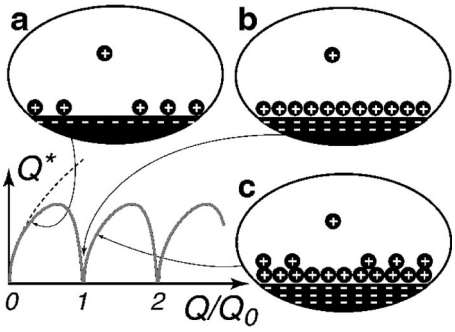

FIG. 10. Inverted charge Q^* as a function of the absolute value Q of the bare charge; Q_0 is the charge of one full layer of Z-ions. The dashed line corresponds to the case of Z-ions with vanishing radius, Eq. (14): (a) The first layer is not full, as in Fig. 6. An approaching new ion creates a correlation hole and is attracted to it. (b) The layer is full, there is no place for a correlation hole. (c) More than one layer is full. A correlation hole exists in the top layer only.

VIII. MULTILAYER ADSORPTION

So far we have not considered the possibility that Z-ions fully cover the macroion surface. This may sometimes happen, particularly when a macroion is very strongly charged or when Z-ions are large. Suppose, for instance, that each Z-ion has a hard core of radius a. In this case, the excluded volume of the hard cores effectively adds positive contributions to the surface pressure and chemical potential of a strongly correlated liquid (10) that are proportional to k_BT and that diverge at full coverage. As the layer approaches full coverage of the macroion surface, this term compensates and then overcompensates for the negative Coulomb term μ_{WC}, so that charge-inversion disappears. Indeed, a full layer is incompressible [see Fig. 10(b)], and, unlike a partially filled layer [see Fig. 6 or Fig. 10(a)], it does not allow for the creation of an imagelike correlation hole.

At even larger macroion charges, a second layer starts to form, launching a new wave of charge-inversion. In the beginning, charge inversion is small because the only attraction of a new Z-ion approaching the surface is provided by a weak interaction with an image in the emerging second layer, where once again $A \gg a$ [Fig. 10(c)]. Continuing, Nguyen and Shklovskii (2001c) arrived at the prediction of an oscillating inverted charge Q^* as a function of Q (see Fig. 10), where charge inversion vanishes every time the top layer of Z-ions is full.

Another way to look at this phenomenon is to examine a metallic electrode screened by Z-ions, when the potential of the electrode is controlled instead of its charge. In this case, oscillations of charge inversion and compressibility lead to oscillations of the capacitance of this electrode with the number of adsorbed layers of Z-ions. This is similar to oscillations of compressibility and magneto-capacitance in the quantum Hall effect, which are related to the consecutive filling of Landau levels (Efros, 1988; Kravchenko *et al.*, 1990; Eisenstein, 1992). In this sense, we are dealing with a classical analog of the quantum Hall effect.

To conclude this section, let us return to the adsorption of weakly charged polyelectrolytes that we discussed briefly in Sec. VII. Dobrynin *et al.* (2001) have shown that parallel chains of adsorbed blobs start touching each other above the same threshold surface charge density $\sigma_e = ef/l^2$, which corresponds to the onset of blobs being squashed on the surface. As a result, these authors arrived at the conclusion that if weakly charged chains are adsorbed on the surface with $\sigma > \sigma_e$, they form a polymer liquid. In this liquid, correlations and image formation are due only to the uppermost layer, with the thickness about that of an unperturbed blob. There are no oscillations of inverted charge; instead, charge-inversion saturates at about one layer of blobs and remains unchanged thereafter.

IX. CORRELATION-INDUCED ATTRACTION OF LIKE CHARGES

The idea of a single screened macroion is a useful one in a theoretical context, but in practice it is rarely true that there is only one macroion. Typically, there is a certain concentration of them, so that interactions between them can be important. Let us start with the simplest question: consider two macroions, and suppose the concentration of Z-ions in solution is equal to N_0 [see Eq. (11)], such that each macroion forms a neutral complex with Z-ions. How do these two neutral complexes interact? It turns out that they attract each other at short distances and therefore tend to coagulate. In other words, two macroions of the same charge may attract each other because of the presence of Z-ions. In general, this attraction of like charges is as interesting a manifestation of correlation as charge inversion. Although our Colloquium emphasizes the phenomenon of charge inversion, we should discuss attraction at least briefly, in order to prepare the ground for the subsequent discussion of experiments (Sec. X).

Medium-induced attraction of like charges is nothing new in physics, with Cooper pairs of electrons being the most prominent example. In the context of molecular physics, the most popular explanation of attraction is in terms of *salt bridges*: a divalent ion, such as Mg^{2+}, can form ionic bonds with two groups with charges of -1 each, in effect connecting them to each other. This idea is indeed adequate if we have, say, two macroion surfaces with regularly placed charges of -1, and there are ions of charge $+2$ between them. However, the bridge concept becomes increasingly fuzzy when Z-ions have charges of 3 or higher and when charges in the macroion are not positioned regularly.

Experimental observations of DNA condensation (see Sec. X) motivated a significant effort by theorists to try to explain attractive forces by going beyond the bridge model. For simplicity, and following the approach taken by the majority of these works, let us consider two planar macroion surfaces with some Z-ions between them. Of course, Poisson-Boltzmann theory predicts pure repulsion for such a system. However, attraction was observed in several computer experiments, including those of Guldbrand *et al.* (1984), Kjellander and Marcelja (1985), Gronbech-Jensen *et al.* (1997), Linse and Lobaskin (1998), and Moreira and Netz (2001). It is important theoretically that, due to dynamic fluctuations of counterions, there is an attractive component (similar to van der Waals interactions), but at effectively high temperature, or small Γ [see Eq. (8) for the definition of Γ], the Poisson-Boltzmann repulsion still dominates and the force remains primarily repulsive (Oosawa, 1968; Lau and Pincus, 1998; Ha and Liu, 1998; Podgornik and Parsegian, 1998; Golestanian *et al.*, 1999; Kardar and Golestanian, 1999; Ha and Liu, 2000).

On the other hand, attraction of like charges dominates at effectively low temperatures, when $\Gamma \gg 1$, and the idea of spatial correlations between Z-ions, which is the central idea of this Colloquium, sheds light on the nature of this attraction. Indeed, for extremely large Γ, we deal with two Wigner crystals on the two opposing plates; they gain energy when they approach each other by properly positioning themselves in the lateral direction. This was shown by Rouzina and Bloomfield (1996; see also Gronbech-Jensen *et al.*, 1997; Levin *et al.*, 1999; Moreira and Netz, 2001). Furthermore, Gronbech-Jensen *et al.* (1997) and Shklovskii (1999a) pointed out that the long-range order of a Wigner crystal is not important for this attractive force. As in the case of charge inversion, what is important is correlation and short-range order. As we know, Z-ions form a strongly correlated liquid (SCL) on the macroion surface as soon as Γ becomes large. Imagine now two planar surfaces, each like Fig. 1, along with their respective SCL's, face to face very close to each other. Clearly, two SCL's merge, lowering the energy per Z-ion from $\varepsilon(n)$ to $\varepsilon(2n) < \varepsilon(n)$ [see Eq. (9)]. Physically, every Z-ion in the merged SCL's is sandwiched between two macroion surfaces, and its Wigner-Seitz cell can be approximated as a pair of disks, one on each surface (compare at Fig. 5). The charge of the cell must still be $-Ze$, but since there are two surfaces, the radius of the cell is reduced by the factor $1/\sqrt{2}$, leading to an energy gain. In some sense, this theory returns us to the idea of bridges, albeit on a completely new level, with each Z-ion bridging between two sides of its Wigner-Seitz cell, which can include many surface charges.

These arguments hold, at least qualitatively, not only for plates, but also for macroions of other shapes, including DNA double helices. More specifically, consider two DNA double helices. When the concentration of Z-ions is equal to N_0, each DNA molecule is neutralized by Z-ions, and the two neutral complexes attract each other at short distances. What happens if the concentration of Z-ions is higher or lower than N_0? In this case, correlation-induced attraction, which is short ranged, competes with Coulomb repulsion, which is much longer ranged. Note that the Coulomb repulsion force is present both at $N < N_0$, when the DNA helices are partially screened by Z-ions and negative, and at $N > N_0$, when they are overcharged and positive.

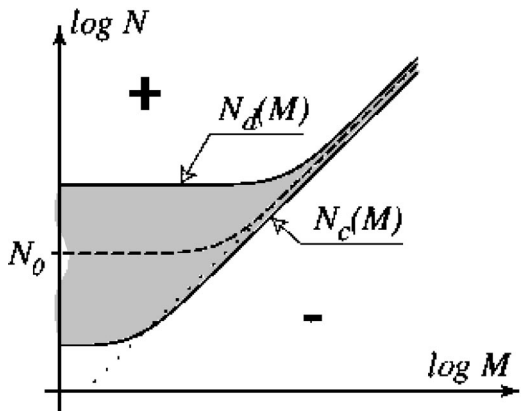

FIG. 11. Generic phase diagram of reentrant condensation and charge inversion in terms of macroion concentration M and Z-ion concentration N (Nguyen and Shklovskii, 2001d). Isoelectric composition is shown by the dotted line. The dashed "neutrality line" corresponds to neutral complexes in the dilute phase. The segregation region is shaded. Minus and plus indicate the signs of complexes of DNA with Z-ions.

What are the implications of this competition between attraction and repulsion? They are summarized in Fig. 11, which shows a phase diagram of the solution with the number concentrations of macroions M, and Z-ions N (along with the neutralizing amount of monovalent ions and salt). The major feature of the phase diagram is the segregation region, which is the shaded area in Fig. 11. As the figure indicates, the generic scenario is that of *reentrant condensation*. DNA molecules stay in solution and remain negative at $N<N_c(M)$, forming undercharged complexes with Z-ions. At some concentration of Z-ions, $N=N_c(M)$, repulsion gives way to the correlation attraction and a condensed phase of DNA is formed, coexisting with a dilute phase. The condensed phase for DNA represents a (nematic) bundle of helices; it exists in the interval $N_c(M)<N<N_d(M)$. Finally, at $N=N_d(M)$, repulsion overcomes the correlation attraction, and the DNA molecules dissolve and form positive (overcharged) complexes with Z-ions.

Inside the coexistence region, there is a neutrality line, at which the equilibrium dilute phase consists of *neutral* complexes. At very small DNA concentrations, the neutrality condition corresponds to the concentration N_0 of Z-ions [Eq. (11)]. To see what happens at larger DNA concentrations, consider increasing M, starting from the overcharged complexes, well above the segregation region in the phase diagram in Fig. 11. When M grows, the solution runs out of Z-ions as it approaches the "isoelectric line" $-\eta LM+ZeN=0$, where $-\eta<0$ is the linear charge density and L is the length of the DNA. Near this line, the charge of the complex flips sign. Thus the neutrality line crosses over from $N=N_0$ to the isoelectric line. The border lines $N_c(M)$ and $N_d(M)$ follow a similar pattern. Although not plotted in Fig. 11, at extremely small values of M these two lines join together at a critical point, and for smaller M only intramolecular condensation of DNA (the coil-globule transition) is possible if the DNA molecule is long enough.

We have considered the phase diagram in Fig. 11 for a solution of DNA chains with small Z-ions. In fact, the diagram is qualitatively quite general (Nguyen and Shklovskii, 2001d). For instance, it applies to a solution of DNA with large positively charged particles. In Sec. VII, we considered the case of a small DNA concentration M, and a large concentration of spheres N, which corresponds to the region above the coexistence region on the phase diagram in Fig. 11. We found that these complexes have the form of necklaces, as shown in Fig. 4, and that they are overcharged, i.e., they contain more spheres than necessary to neutralize the DNA molecule. The large spheres are so strongly bound to the DNA that the concentration N_0 for them is extremely small, and any real experiment deals with the narrow upper-right part of the diagram. Suppose now that there are relatively few spheres in the solution, so that we are below the neutrality line. In this situation, chains make an overcharging number of turns around each sphere. This is energetically favored due to the repulsive correlations between subsequent turns on a sphere surface. The inverted net charge of each sphere is about as large as for the case of a single sphere, as discussed in Sec. VII. Furthermore, the inverted charge of the spheres determines their distribution along the chain of polyelectrolyte. Negative spheres repel each other, and therefore the complex once again has the periodic beads-on-a-string structure shown in Fig. 4, which resembles the 10-nm chromatin fiber. In the narrow vicinity of the neutrality line, even a small correlation attraction between touching spheres is sufficient to drive aggregation (or coil-globule collapse for long chains) of DNA with spheres.

X. EXPERIMENTAL EVIDENCE OF CHARGE INVERSION

How does the theory of correlated screening compare with experiment? For the purposes of this Colloquium, we restrict ourselves solely to a qualitative comparison.

First observations of charge inversion were reported a long time ago by Bungenberg de Jong (1949). He was able to measure electrophoresis of macroscopic aggregates in the phase segregation region of the phase diagram in Fig. 11 and observed the reverse of their mobility upon crossing the isoelectric line. More recently, Kabanov and co-workers (Kabanov and Kabanov, 1995, 1998; Kabanov *et al.*, 1996) examined mixtures of positive and negative polymers and directly observed interpolyelectrolyte complexes in which a larger polymer of one sign (playing the role of a macroion) was seen to bind an overcharging amount of smaller polymers of the opposite sign (playing the role of Z-ions). The effect was directly seen due to the reversal of electrophoretic mobility of the complexes. Furthermore, Wang *et al.* (1999) observed a similar reversal for a mixture of polyelectrolytes (macroions) and micelles (Z-ions). Gotting *et al.* (1999) found reversed mobility for nanoparticles (macroions) and short single-stranded DNA (elongated Z-ions). Walker and Grant (1996) demonstrated this phenomenon for 120-nm latex particles (macroions) with

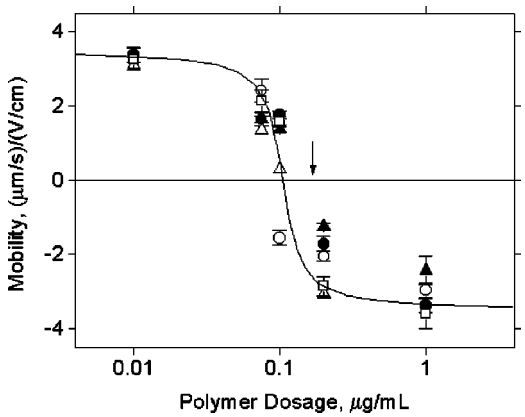

FIG. 12. Mobility of positive latex particles (macroions) in the presence of 0.005 M (moles per liter) concentration of NaCl as a function of polymer mass concentration. Polymers (single-stranded DNA chains) play the role of Z-ions. Different symbols correspond to DNA of the following lengths (in monomers): ▲, 8; ○, 10; △, 40; ●, 80; □, 1400. The line is drawn to guide the eye. The arrow indicates the isoelectric point, the polymer mass concentration of 0.17 μg ml^{-1} at which the DNA charge neutralizes the latex particles.

single-stranded DNA (Z-ions) ranging from 8 to 1400 nucleotides; their data are presented in Fig. 12. Kabanov *et al.* (2000) and Evans *et al.* (2001) observed reversed electrophoretic mobility for DNA with dendrimers playing the role of Z-ions.

An interesting observation, apparent from Fig. 12, is that, upon rescaling, the data for different DNA lengths collapse onto a single master curve (in which mobility is plotted against mass concentration of DNA instead of number concentration N). A possible reason for this is that the isoelectric point is determined by the number of charged groups per unit volume, but this quantity is insensitive to the overall length of DNA and is simply proportional to the mass concentration.

All of the above-mentioned experimental works rely on the reverse of electrophoretic mobility as an indication of charge inversion. Indeed, this is conceptually the most straightforward approach. It is valid because Z-ions are strongly bound to the macroion, with energies larger than k_BT, and move together with it. On the other hand, monovalent ions screening the net charge Q^* are attracted to macroions with an energy much smaller than k_BT and move in an electric field in the opposite direction. For these reasons, it is the net charge Q^* that determines both the magnitude and the sign of the observed electrophoretic mobility. This is also the case when monovalent ions adsorb on Z-ions, effectively reducing them to Z'-ions with $Z'<Z$, as shown in Fig. 7. In all cases, the net charge includes all ions bound with energies in excess of k_BT. In a recent molecular dynamics simulation, Tanaka and Grosberg (2001b) have directly examined the mobility of charge-inverted macroion complexes similar to the one shown in Fig. 7. They confirmed that adsorbed Z-ions drift together with the macroion in a weak electric field and that the sign of the net charge Q^* determines the direction of electrophoresis.

It is also worth mentioning that the interpretation of electrophoretic experiments on charge inversion is not affected by the recent discoveries of Long *et al.* (1996, 1998). These authors noted that electrophoretic mobility, under some circumstances, may not be entirely determined by the charge. For instance, even an overall neutral object may move in an electric field provided that it has a strongly asymmetric charge distribution. A simple example consists of two balls of different radii, rigidly connected by a thin rod, and having opposite charges. The effect is due to the fact that an external electric field acts not only on the macroion itself, but also on surrounding co- and counterions, causing the latter to flow and to exert viscous friction drag forces on the macroion. A strong geometrical asymmetry of positive and negative charges leaves these drag forces unbalanced. In this Colloquium, we discuss only macroions in which the bare charge is uniformly distributed on the surface. In this case, the charge of the Z-ions is practically uniform, too (except over small length scales of the order of R, the distance between neighboring adsorbed Z-ions). For such macroions, reversal of electrophoretic mobility does indeed indicate an inversion of charge.

For a more detailed comparison with experiment, we should remember that charge reversal is expected to be accompanied by coagulation, as discussed above in Sec. IX. Whether in equilibrium or not quite in equilibrium, these large complexes should scatter light strongly. There are many experiments reporting such observations.

Let us begin with DNA. It has been known for some time that at some critical concentration of Z-ions, N_c, DNA abruptly condenses into large bundles (Bloomfield, 1996, 1998). Recently it was discovered that at a much larger critical concentration, N_d, the bundles dissolve back (Pelta, Durand, *et al.*, 1996a; Pelta, Livolant, *et al.*, 1996b; Raspaud *et al.*, 1998, 1999; Saminathan *et al.*, 1999). Specifically, for the spermine ions ($Z=4$), it was found experimentally that $N_c=0.025$ mM and $N_d=150$ mM. If one interprets these data in the framework of the theory of Nguyen *et al.* (2000), the experimental values of N_c and N_d imply that, for spermine, $N_0=3.2$ mM and the binding energy of two helices per one spermine ion is $u=0.3k_BT$. The last value agrees with one obtained by a different method (Rau and Parsegian, 1992).

Let us now discuss some other systems. Wang *et al.* (1999) studied complex formation in a mixture of micelles and oppositely charged polyelectrolytes. In this experiment, the total charge of micelles was controlled by changing the concentration of the cationic lipid in the solution. In agreement with the above theory, measurements of dynamic light scattering and turbidity (coefficient of light scattering) show that complexes condense in bundles and the solution coacervates in the vicinity of the point where the mobility crosses over between two almost constant values, positive and negative.

For complexes of latex particles with DNA of various lengths, examined by Walker and Grant (1996), equilibrium conditions were not found, but the latex particles

showed a significant rate of aggregation in the same narrow range of DNA concentrations where the mobility flips its sign.

There is a large body of interesting experimental (Rädler *et al.*, 1997; Koltover *et al.*, 1999) and theoretical (Bruinsma, 1998; Harries *et al.*, 1998) work on phase diagrams and overcharging of lamellar cationic lipid-DNA self-assembled complexes. These solutions always seem to have aggregates due to hydrophobic attraction of lipids. A phase diagram of this kind has been sketched by Rädler (2000).

Another large body of work with a technologically useful example of overcharging deals with the sequential adsorption of multiple layers of polyelectrolytes of alternating sign [see Decher (1997) and references therein]. For example, a positive surface is first treated with negative polymers, gets overcharged, and becomes negative; it is then treated with positive polymers, gets overcharged, etc. This procedure works reliably up to many tens of layers. A theoretical interpretation of this technique was discussed by Castelnovo and Joanny (2000). This goes beyond the scope of the present Colloquium however, as it involves certain kinetic considerations, while we deal here only with equilibrium phenomena.

XI. CORRELATIONS "IN SHEEP'S CLOTHING"

We have mentioned correlations so many times in this Colloquium that the reader may want to ask: Are there alternative, correlation-independent, electrostatic mechanisms leading to charge inversion? Our answer is no, and we argue that the correlation-based mechanism is the universal one. This fact notwithstanding, we should say that correlations may show up in a number of ways, sometimes disguised like a wolf in sheep's clothing.

To understand better the role of correlations, let us first consider the case of no correlation. Suppose we have a set of randomly positioned pointlike charges, with equal numbers of $+e$ and $-e$. It is easy to establish that the averaged interaction energy in such a system is exactly zero, where the average is taken over independent random positions of all charges. Similarly, the averaged electric field in the system is also zero. Both of these statements remain correct for a one-component plasma, in which pointlike charges of one sign are randomly positioned on the smeared uniform background of the opposite sign.

The essence of screening is that charges in plasma are *not* positioned randomly. Correlations happen because ions reconfigure themselves nonrandomly to gain some energy. This so-called correlation energy is well known in plasma physics (Landau and Lifshitz, 1977). It is negative, meaning that a correlated configuration is lower in energy, or more thermodynamically favored, than a random configuration.

These simple facts allow us to understand the underlying role of correlations in one of the theories suggested in the literature to explain charge inversion. This theory, put forward by Park *et al.* (1999) views monovalent *counterion release* from Z-ions as the driving force behind charge inversion. We argue that while counterion release occurs, it is itself driven by correlations. Once again let us imagine that DNA molecules, along with their Onsager-Manning-condensed small ions, are being adsorbed on the macroion one at a time (possibly releasing some of their counterions). Let us further consider the moment when neutralization has just been achieved. Pretend now that DNA rods (Z-ions) are distributed randomly on the surface, uncorrelated in both position and orientation. In this case, the next arriving DNA molecule feels no average field, so that it has no reason to release its counterions. The situation is completely different if DNA molecules are correlated on the surface (see Figs. 2 or 8), where locally each molecule is surrounded by a correlation hole—the positive stripe of the background charge (the Wigner-Seitz cell). The corresponding field, or the positive potential of the Wigner-Seitz cell, causes the release of counterions from DNA not only at the neutrality point, but even if the surface overall is overcharged [see the solution of this problem given by Eqs. (20) and (21)]. These qualitative arguments can be formulated more quantitatively (Nguyen *et al.*, 2001). Thus the correlation hole (or the adjustment of DNA molecules to each other, or the image charge, or correlations—all are synonyms!) is the driving force for *both* counterion release *and* charge inversion; under the sheep's clothing of counterion release, there is a wolf's face of correlations.

Let us now discuss another approach, which we call *metallization*. It was pioneered by Mateescu *et al.* (1999), who considered formation of complexes made up of polyelectrolyte molecules and oppositely charged spheres, and by Joanny (1999), who examined adsorption of flexible polymers on a charged plane. Metallization theory considers adsorbed Z-ions as a continuous medium similar to a metal, while still treating the bulk solution as consisting of discrete charges.

We argue that metallization theory is in fact an overestimate of correlation effects. Indeed, as shown in Fig. 6, a strongly correlated liquid behaves as a metal on the length scale above R, the distance between neighboring adsorbed Z-ions. It behaves as a metal in the sense that it responds to the approaching new Z-ion by forming an image. Clearly, the smeared continuum is also a metal in this sense, and even a better metal—it is a metal on all length scales. Another way to view this same physics is to note that correlation suppresses the electric field of every Z-ion beyond a certain distance of order R, while for the smeared continuum the field is suppressed everywhere, and therefore the effect is overestimated.

The latter view also suggests another fruitful interpretation of the metallization approach in terms of the self-energy of Z-ions. Here, we resort to the terminology in which the self-energy of an ion is identified with the energy of the electric field outside a certain cutoff length, such as an ion size. (We are not interested in the electric field on smaller length scales: although the energy of this field is infinite, it does not change as a result

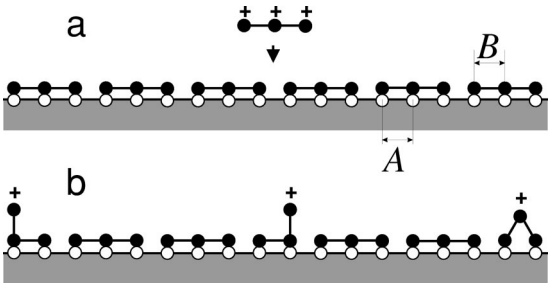

FIG. 13. Schematic representation of charge fractionalization: (a) One strand of negative charges of DNA (empty balls) is completely neutralized by positive Z-ions with $Z=3$. Their charged groups are shown by black balls. A new Z-ion is approaching. (b) The new Z-ion is "digested." Its charge is split in $+e$ charges of Z defects, tails, and arches.

of any processes considered here, such as adsorption of Z-ions.) Using this language, the metallization theory becomes physically transparent. Indeed, in this theory adsorption of Z-ions is energetically favored because they do have self-energy while in the bulk solution and lose it completely upon adsorption. Once again, real screening, or correlations between Z-ions, corresponds to the suppression of a part of the self-energy, corresponding to the energy of the electric field beyond a distance of order R. The energy of the field between the ion size and R is the amount of overestimation by the metallization theory. In contrast, the Poisson-Boltzmann approximation fails to describe charge inversion precisely because it smears Z-ions everywhere and neglects their self-energies.

The representation of correlations in terms of self-energy allows us to address one more problem of practical importance, namely, the discreteness of charges (Nguyen and Shklovskii, 2002). Indeed, instead of a uniformly charged surface, as in Fig. 1, it would be closer to reality (and to a chemist's heart) to think of a macroion as having some charged groups, each with unitary charge. For instance, negative $(-e)$ charges of DNA are positioned on an external spiral rim of the double helix, at a distance $A=0.67$ nm from each other along the rim.

To be specific, let us consider a macroion that is a regular lattice of charges $-e$ (an "unfolded DNA strand") and a Z-ion having a linear array of charges $+e$ (a short polyelectrolyte). Importantly, Z-ions always have some degree of flexibility; for instance, in the case $Z=3$, as shown in Fig. 13, we can imagine that they freely bend in the middle. For simplicity we assume that the distance B between charges in the Z-ion matches exactly that in the macroion, A: $A=B$. Finally, we assume that the charges of the Z-ion and the macroion can approach each other to a minimal distance much smaller than A. Then Z-ions can attach to the macroion, locally compensating for each charge, and therefore achieving complete neutralization, as shown in Fig. 13(a). The neutralization is so perfect that it is difficult to imagine how another Z-ion could be attached. Figure 13 explains why this happens. Suppose that the macroion is already neutralized by Z-ions and a new Z-ion comes along similar to Fig. 6. Then it turns out to be energetically favored for the system to form Z defects in Z independent places in the ordered array of neutralizing Z-ions, thus creating room for a new Z-ion. In each defect, one charge of the Z-ion is detached from the corresponding macroion charge, forming a positive tail or arch above the surface and leaving a negative vacancy on the macroion. When Z-ions are shifted along the macroion, Z vacancies can then join together and form a large vacancy capable of accommodating an entire new Z-ion. The net result is that Z disconnected charges $+e$ appear on top of the completely neutralized macroion [Fig. 13(b)], or, in other words, the charge of the Z-ion is fractionalized. To avoid misunderstanding, we emphasize that none of the chemical bonds is really cut.

Fractionalization effectively eliminates the self-energy of the free Z-ion. Indeed, the self-energy of the Z-ion is simply the energy of repulsion between Z positive-constituent charged groups in the extended conformation which the Z-ion assumes in the solution. In the fractionalized state, charges are far apart and practically do not interact, so that self-energy is gained. These results are easily generalized for the case $B<A$, when Z-ions have larger linear charge density than the macroion. For instance, if $B=A/2$, then Z-ions repelling each other form a "Wigner crystal" on top of the lattice of macroion charges, where they alternate with vacant places (similarly to Figs. 1, 5, 6, and 8).

Is fractionalization a correlation-independent mechanism of charge inversion? Of course not: this phenomenon is solely due to the correlated distribution of Z-ions, which avoid each other at the macroion. Fractionalization is yet another mask under which correlations may show up.

XII. CHARGE INVERSION IN A BROADER PHYSICS CONTEXT

The charge inversion studied in this Colloquium has many physical analogies. There are other "charge-inverted" systems in physics. Let us start with the hydrogen atom. It is known that it can bind a second electron, forming the negative ion H^- with an ionization energy of approximately 0.05 Ry (Massey, 1938). We can consider this effect as the inversion of proton charge. Attraction of the second electron to the neutral atom is due to the Coulomb correlation between electrons: the first electron avoids the second one, spending more time on the opposite side of the proton. In other words, binding is related to polarization of the neutral core.

Negative ions—nuclei overcharged by electrons—also exist for larger atoms. Mean-field Thomas-Fermi or Hartree theories fail to explain negative ions (Landau and Lifshitz, 1980). One must include exchange and Coulomb correlation holes to arrive at a satisfactory theory explaining the bound state and the nonzero ionization energy of a negative ion (Massey, 1938). The Thomas-Fermi theory of an atom is an analog of the Poisson-Boltzmann theory of electrolytes. It is not surprising that both fail to explain charge-inverted states.

Similar considerations also apply for a macroscopic metallic particle. Electrons in such a particle have a negative chemical potential (compared to a vacuum) or, in other words, a positive work function. The work function is known to vanish in the Thomas-Fermi or Hartree approximations (Lang, 1973).

The energy $|\mu_{WC}|$ plays the same role for Z-ions on the insulating macroion surface as the ionization energy of a negative ion or the work function of a metallic particle for electrons. Similarly to electrons, charge inversion of a charged insulating macroion by Z-ions cannot be obtained in the mean-field Poisson-Boltzmann approximation. Only correlations of Z-ions on the surface of the macroion can lead to charge inversion.

Let us now return to Onsager-Manning condensation (Manning, 1969; Sec. II). Kosterlitz and Thouless (1972, 1973) discovered a similar threshold phenomenon for the generation of free vortexes in two-dimensional superfluids or superconductors. They noticed that, due to the logarithmic form of attractive interaction, two vortexes of opposite sign decouple only above some critical temperature T_{KT}. Later, Kosterlitz-Thouless theory was applied to the unbinding of dislocations and disclinations in the theory of defect-induced melting of two-dimensional crystals (Nelson and Halperin, 1979; Young, 1979).

In the Kosterlitz-Thouless theory, one can identify an analog of the short-range correlation contribution to the chemical potential of Z-ions (which we call $|\mu_{WC}|$). This is the energy of creation of the two vortex cores. As in $|\mu_{WC}|$, this energy provides additional binding of vortexes and strongly reduces the concentration of free vortexes at $T>T_{KT}$ (Minnhagen, 1987). In contrast to the Kosterlitz-Thouless theory, the short-range contribution $|\mu_{WC}|$ was only recently introduced (Perel and Shklovskii, 1999).

Another physical analogy already mentioned in Sec. VIII is the integer quantum Hall effect. We should add that charge fractionalization, as illustrated by Fig. 13, is an analog of the fractional quantum Hall effect (Prange and Girvin, 1990). Finally, Fig. 13 also bears a resemblance to electron charge fractionalization in polyacetylene (Brazovskii and Kirova, 1991).

XIII. CONCLUSIONS AND OUTLOOK

We have discussed the physical picture of screening for the case of strongly interacting ions. This case appears to have been overlooked for many decades, since Debye. Its theoretical study, motivated mainly by experiments on gene delivery and chromatin structure, has revealed new and interesting physical insights. Specifically, correlations between screening ions lead to such counterintuitive phenomena as charge inversion, reverse electrophoretic mobility, attraction of like-charged molecules or colloids, etc. The physical theory of these phenomena is aesthetically attractive, as it presents many parallels with other areas of physics, ranging from the quantum Hall effect to atomic physics and the physics of metals. The potential applications are many, in both chemical and biological realms. They include all sorts of manipulations with DNA, both for biological purposes and as an assembly tool for nonbiological nanotechnology. All require an understanding of the electrostatic properties of DNA chains. Many diseases have to do with mis-assemblies of charged proteins such as actin; we need to understand better the assembly of such objects. Food, cosmetics, paper, and waste-water treatment industries are all about charged colloids, and the list of applications is easy to continue. In brief, this theory is one of the busy junctions where physics meets chemistry and biology.

ACKNOWLEDGMENTS

We have enjoyed collaborations with V. I. Perel, I. Rouzina, and M. Tanaka. We are grateful to V. Bloomfield, E. Braun, R. Bruinsma, P. Chaikin, A. Dobrynin, P. Dubin, M. Dyakonov, W. Gelbart, S. Girvin, W. Halley, C. Holm, J.-F. Joanny, A. Kabanov, V. Kabanov, A. Khokhlov, R. Kjellander, K. Kremer, A. Koulakov, V. Lobaskin, F. Livolant, D. Long, G. Manning, R. Netz, P. Pincus, R. Podgornik, E. Raspaud, M. Rubinstein, J.-L. Sikorav, U. Sivan, M. Voloshin, and J. Widom for useful discussions. We thank Zhifeng Shao for permission to use Figs. 2 and 3, and S. Grant for permission to use Fig. 12. T.T.N. and B.I.S. were supported by NSF DMR-9985785.

REFERENCES

Andelman, D., and J.-F. Joanny, 2000, C. R. Acad. Sci. (Paris) **1**, 1153.
Aberts, B., D. Bray, J. Lewis, M. Raff, K. Roberts, and J. D. Watson, 1994, *Molecular Biology of the Cell* (Galland Publishing, New York).
Bloomfield, V. A., 1996, Curr. Opin. Struct. Biol. **6**, 334.
Bloomfield, V. A., 1998, Biopolymers **44**, 269; Chap. 7 at http://biosci.umn.edu/biophys/BTOL/supramol.html
Bjerrum, N. J., 2000, Z. Phys. Chem. (Munich) **119**, 145.
Braun, E., Y. Eichen, U. Sivan, and G. Ben-Yoseph, 1998, Nature (London) **391**, 775.
Brazovskii, S., and N. Kirova, 1991, JETP Lett. **33**, 4.
Bruinsma, R., 1998, Eur. Phys. J. B **4**, 75.
Bungenberg de Jong, M. G., 1949, in *Colloid Science*, edited by H. R. Kruyt (Elsevier, New York), p. 335.
Castelnovo, M., and J.-F. Joanny, 2000, Langmuir **16**, 7524.
Chapman, D., 1913, Philos. Mag. **25**, 475.
Chodanowski, P., and S. Stoll, 2001, Macromolecules **34**, 2320.
Debye, P., and E. Hückel, 1923, Phys. Z. **24**, 185.
Decher, G., 1997, Science **277**, 1232.
de Gennes, P.-G., P. Pincus, R. M. Velasco, and F. Brochard, 1976, J. Phys. (Paris) **37**, 1461.
Dobrynin, A. V., A. Deshkovski, and M. Rubinstein, 2001, Macromolecules **34**, 3421.
Efros, A. L., 1988, Solid State Commun. **65**, 1281.
Eisenstein, J. P., L. N. Pfeifer, and K. W. West, 1992, Phys. Rev. Lett. **68**, 674.
Ennis, J., S. Marcelja, and R. Kjellander, 1996, Electrochim. Acta **41**, 2115.

Evans, H. M., A. Ahmad, T. Pfohl, A. Martin, and C. R. Safinya, 2001, Bull. Am. Phys. Soc. **46**, 391.
Fang, Y., and J. Yang, 1997, J. Phys. Chem. B **101**, 441.
Felgner, P. L., 1997, Sci. Am. **276**, 102.
Frank-Kamenetskii, M. D., V. V. Anshelevich, and A. V. Lukashin, 1987, Sov. Phys. Usp. **30**, 317.
Gelbart, W., R. Bruinsma, P. Pincus, and A. Parsegian, 2000, Phys. Today **53** (9), 38.
Golestanian, R., M. Kardar, and T. B. Liverpool, 1999, Phys. Rev. Lett. **82**, 4456.
Götting, N., H. Fritz, M. Maier, J. von Stamm, T. Schoofs, and E. Bayer, 1999, Colloid Polym. Sci. **277**, 145.
Gouy, G., 1910, J. Phys. Radium **9**, 457.
Gronbech-Jensen, N., R. J. Mashl, R. F. Bruinsma, and W. M. Gelbart, 1997, Phys. Rev. Lett. **78**, 2477.
Guldbrand, L. G., Bo Jonsson, H. Innerstrom, and P. Linse, 1984, J. Chem. Phys. **80**, 2221.
Ha, B.-Y., and A. J. Liu, 1998, Phys. Rev. Lett. **81**, 1011.
Ha, B.-Y., and A. J. Liu, 2000, in *Physical Chemistry of Polyelectrolytes*, edited by T. Radeva (Dekker, New York), p. 163.
Harries, D., S. May, W. M. Gelbart, and A. Ben-Shaul, 1998, Biophys. J. **75**, 159.
Joanny, J.-F., 1999, Eur. Phys. J. B **9**, 117.
Kabanov, V. A., V. P. Evdakov, M. I. Mustafaev, and A. D. Antipina, 1976, Mol. Biol. (Moscow) **11**, 52.
Kabanov, A. V., and V. A. Kabanov, 1995, Bioconjugate Chem. **6**, 7.
Kabanov, A. V., and V. A. Kabanov, 1998, Adv. Drug Delivery Rev. **30**, 49.
Kabanov, V. A., V. G. Sergeyev, O. A. Pyshkina, A. A. Zinchenko, A. B. Zezin, J. G. H. Joosten, J. Brackman, and K. Yoshikawa, 2000, Macromolecules **33**, 9587.
Kabanov, V. A., A. A. Yaroslavov, and S. A. Sukhisvili, 1996, J. Controlled Release **39**, 173.
Kardar, M., and R. Golestanian, 1999, Rev. Mod. Phys. **71**, 1233.
Katzir-Katchalsky, A., 1971, *Biophysics and Other Topics: Selected Papers* (Academic, Orlando).
Keren, K., Y. Soen, G. Ben Yoseph, R. Yechieli, E. Braun, U. Sivan, and Y. Talmon, 2002, unpublished.
Kjellander, R., and S. Marcelja, 1985, Chem. Phys. Lett. **114**, 124(E).
Koltover, I., T. Salditt, and C. R. Safinya, 1999, Biophys. J. **77**, 915.
Kosterlitz, J. M., and D. J. Thouless, 1972, J. Phys. C **5**, L124.
Kosterlitz, J. M., and D. J. Thouless, 1973, J. Phys. C **6**, 1181.
Kravchenko, S. V., D. A. Rinberg, S. G. Semenchinsky, and V. Pudalov, 1990, Phys. Rev. B **42**, 3741.
Landau, L. D., and E. M. Lifshitz, 1977, *Statistical Physics, Part 1* (Pergamon, Oxford), Chap. VII.
Landau, L. D., and E. M. Lifshitz, 1980, *Quantum Mechanics (Nonrelativistic Theory)* (Pergamon, Oxford), Chap. X.
Lang, N. D., 1973, in *Solid State Physics*, edited by H. Ehrenreich, F. Seitz, and D. Turnbull (Academic, New York), Vol. 28, p. 225.
Lau, A. W. C., and P. A. Pincus, 1998, Phys. Rev. Lett. **81**, 1338.
Levin, Y., J. J. Arenzon, and J. F. Stilck, 1999, Phys. Rev. Lett. **83**, 2680.
Linse, P., and V. Lobaskin, 1998, Phys. Rev. Lett. **83**, 4208.
Long, D., A. V. Dobrynin, M. Rubinstein, and A. Ajdari, 1998, J. Chem. Phys. **108**, 1234.
Long, D., J.-L. Viovy, and A. Ajdari, 1996, Phys. Rev. Lett. **76**, 3858.
Luger, K., A. Mader, R. Richmond, D. Sargent, and T. Richmond, 1997, Nature (London) **389**, 251. For pictures visit, for example, http://info.bio.cmu.edu/Courses/03438/Nsome/1AOI.htm
Manning, G. S., 1969, J. Chem. Phys. **51**, 924.
Massey, H. S. W., 1938, *Negative Ions* (Cambridge University Press, Cambridge).
Mateescu, E. M., C. Jepperseni, and P. Pincus, 1999, Europhys. Lett. **46**, 454.
Messina, R., C. Holm, and K. Kremer, 2000a, Phys. Rev. Lett. **85**, 872.
Messina, R., C. Holm, and K. Kremer, 2000b, Europhys. Lett. **51**, 461.
Minnhagen, P., 1987, Rev. Mod. Phys. **59**, 1001.
Moreira, A. G., and R. R. Netz, 2000, Europhys. Lett. **52**, 705.
Moreira, A. G., and R. R. Netz, 2001, Phys. Rev. Lett. **87**, 078301.
Moreira, A. G., and R. R. Netz, 2002, Europhys. Lett. **57**, 911.
Mou, J., D. M. Czajkowsky, Y. Zhang, and Z. Shao, 1995, FEBS Lett. **371**, 279.
Nelson, D. R., and B. I. Halperin, 1979, Phys. Rev. B **19**, 2457.
Netz, R. R., and J.-F. Joanny, 1999a, Macromolecules **32**, 9013.
Netz, R. R., and J.-F. Joanny, 1999b, Macromolecules **32**, 9026.
Nguyen, T. T., A. Yu. Grosberg, and B. I. Shklovskii, 2000a, Phys. Rev. Lett. **85**, 1568.
Nguyen, T. T., A. Yu. Grosberg, and B. I. Shklovskii, 2000b, J. Chem. Phys. **113**, 1110.
Nguyen, T. T., A. Yu. Grosberg, and B. I. Shklovskii, 2001, in *Electrostatic Effects in Soft Matter and Biophysics*, Proceedings of the NATO Advanced Study Institute, Les Houches, France, 2000, edited by C. Holm, P. Kekicheff, and R. Podgornik, NATO Science Series: II: Mathematics, Physics and Chemistry, No. 46 (Kluwer Academic, Dordrecht), p. 469.
Nguyen, T. T., I. Rouzina, and B. I. Shklovskii, 2000, J. Chem. Phys. **112**, 2562.
Nguyen, T. T., and B. I. Shklovskii, 2001a, Physica A **293**, 324.
Nguyen, T. T., and B. I. Shklovskii, 2001b, J. Chem. Phys. **114**, 5905.
Nguyen, T. T., and B. I. Shklovskii, 2001c, Phys. Rev. E **64**, 041407.
Nguyen, T. T., and B. I. Shklovskii, 2001d, J. Chem. Phys. **115**, 7298.
Nguyen, T. T., and B. I. Shklovskii, 2002, Physica A (in press), cond-mat/0109002.
Onsager, L., 1967, private communication to G. Manning.
Oosawa, F., 1968, Biopolymers **6**, 134.
Oosawa, F., 1971, *Polyelectrolytes* (Dekker, New York).
Pan, J., D. Thirumalai, and S. Woodson, 1999, Proc. Natl. Acad. Sci. U.S.A. **96**, 6149.
Park, S. Y., R. F. Bruinsma, and W. M. Gelbart, 1999, Europhys. Lett. **46**, 493.
Pelta, J., D. Durand, J. Doucet, and F. Livolant, 1996, Biophys. J. **71**, 48.
Pelta, J., F. Livolant, and J.-L. Sikorav, 1996, J. Biol. Chem. **271**, 5656.
Perel, V. I., and B. I. Shklovskii, 1999, Physica A **274**, 446.
Podgornik, R., and V. A. Parsegian, 1998, Phys. Rev. Lett. **80**, 1560.
Potemkin, I. I., K. B. Zeldovich, and A. R. Khokhlov, 2000, Polym. Sci., Ser. C **42**, 154.
Prange, R. E., and S. M. Girvin, Eds., 1990, *The Quantum Hall Effect*, 2nd ed. (Springer, Heidelberg).

Rädler, J. O., I. Koltover, T. Saddit, and C. R. Safinya, 1997, Science **275**, 810.
Rädler, J. O., 2000, in *Electrostatics Effects in Biophysics and Soft Matter*, edited by C. Holm, P. Kekicheff, and R. Podgornik (Kluwer Academic, Dordrecht).
Raspaud, E., M. Olvera de la Cruz, J.-L. Sikorav, and F. Livolant, 1998, Biophys. J. **74**, 381.
Raspaud, E., I. Chaperon, A. Leforestier, and F. Livolant, 1999, Biophys. J. **77**, 1547.
Rau, D. C., and A. V. Parsegian, 1992, Biophys. J. **61**, 246.
Rouzina, I., and V. A. Bloomfield, 1996, J. Phys. Chem. **100**, 9977.
Saminathan, M., T. Antony, A. Shirahata, L. Sigal, T. Thomas, and T. J. Thomas, 1999, Biochemistry **38**, 3821.
Sens, P., and E. Gurovitch, 1999, Phys. Rev. Lett. **82**, 339.
Shao, Z., 1999, News Physiol. Sci. **14**, 142.
Shklovskii, B. I., 1999a, Phys. Rev. Lett. **82**, 3268.
Shklovskii, B. I., 1999b, Phys. Rev. E **60**, 5802.
Tanaka, M., and A. Yu. Grosberg, 2001a, J. Chem. Phys. **115**, 567.
Tanaka, M., and A. Yu. Grosberg, 2001b, preprint cond-mat/0106561.
Tang, M. X., C. T. Rederman, and F. C. Szoka, Jr., 1996, Bioconjugate Chem. **7**, 703.
Terao, T., and T. Nakayama, 2001, Phys. Rev. E **63**, 041401.
Totsuji, H., 1978, Phys. Rev. A **17**, 399.
Walker, H. W., and S. B. Grant, 1996, Colloids Surf., A **119**, 229.
Wallin, T., and P. Linse, 1996, J. Phys. Chem. **100**, 17873.
Wallin, T., and P. Linse, 1997, J. Phys. Chem. **101**, 5506.
Wang, Y., K. Kimura, Q. Huang, P. L. Dubin, and W. Jaeger, 1999, Macromolecules **32**, 7128.
Woodson, S., 2000, Nat. Struct. Biol. **7**, 349.
Xia, J., and P. L. Dubin, 1994, in *Macromolecular Complexes in Chemistry and Biology*, edited by P. L. Dubin *et al.* (Springer-Verlag, Berlin)
Young, A., 1979, Phys. Rev. B **19**, 1855.
Zimm, B., and M. Le Bret, 1983, J. Biomol. Struct. Dyn. **1**, 461.